1998

New Rotation Periods in the Pleiades: Interpreting Activity Indicators

Anita Krishnamurthi
Ohio State University

D. M. Terndrup
Ohio State University

M. H. Pinsonneault
Ohio State University

See next page for additional authors

Krishnamurthi, Anita, et al. New Rotation Periods in the Pleiades: Interpreting Activity Indicators. The Astrophysical Journal (1998) 493:914.

New Rotation Periods in the Pleiades: Interpreting Activity Indicators

Abstract
We present results of photometric monitoring campaigns of G, K and M dwarfs in the Pleiades carried out in 1994, 1995 and 1996. We have determined rotation periods for 18 stars in this cluster. In this paper, we examine the validity of using observables such as X-ray activity and amplitude of photometric variations as indicators of angular momentum loss. We report the discovery of cool, slow rotators with high amplitudes of variation. This contradicts previous conclusions about the use of amplitudes as an alternate diagnostic of the saturation of angular momentum loss. We show that the X-ray data can be used as observational indicators of mass-dependent saturation in the angular momentum loss proposed on theoretical grounds.

Keywords
Star activity, star evolution, star rotation, star spots, star X-rays

Disciplines
Astrophysics and Astronomy | Stars, Interstellar Medium and the Galaxy

Authors
Anita Krishnamurthi, D. M. Terndrup, M. H. Pinsonneault, K. Sellgren, John R. Stauffer, Rudolph Schild, D. E. Backman, K. B. Beisser, D. B. Dahari, Amil Dasgupta, J. T. Hagelgans, M. A. Seeds, Rajan Anand '98, Bentley D. Laaksonen '95, Laurence A. Marschall, and T. Ramseyer

To appear in *The Astrophysical Journal*

New rotation periods in the Pleiades: Interpreting activity indicators

Anita Krishnamurthi[1],[2], D. M. Terndrup[1], M. H. Pinsonneault and K. Sellgren
Department of Astronomy, The Ohio State University, 174 W. 18th Ave., Columbus, OH 43210
Electronic mail: anita,terndrup,pinsono,sellgren@astronomy.ohio-state.edu

John R. Stauffer and Rudolph Schild
Smithsonian Astrophysical Observatory, 60 Garden St., Cambridge, MA 02138
Electronic mail: stauffer@cfa.harvard.edu, rschild@cfa.harvard.edu

D. E. Backman, K. B. Beisser, D. B. Dahari, A. Dasgupta, J. T. Hagelgans and M. A. Seeds
Dept. of Physics and Astronomy, Franklin and Marshall College, P.O. Box 3003, Lancaster, PA 17604
Electronic mail: dana@astro.fandm.edu, m_seeds@acad.fandm.edu

Rajan Anand, Bentley D. Laaksonen, Laurence A. Marschall and T. Ramseyer
Dept. of Physics, Gettysburg College, Gettysburg, PA 17325
Electronic mail: marschal@gettysburg.edu, ramseyer@goethe.uca.edu

ABSTRACT

We present results of photometric monitoring campaigns of G, K and M dwarfs in the Pleiades carried out in 1994, 1995 and 1996. We have determined rotation periods for 18 stars in this cluster. In this paper, we examine the validity of using observables such as X-ray activity and amplitude of photometric variations as indicators of angular momentum loss. We report the discovery of cool, slow rotators with high amplitudes of variation. This contradicts previous conclusions about the use of amplitudes as an alternate diagnostic of the saturation of angular momentum loss. We show that the X-ray data can be used as observational indicators of mass-dependent saturation in the angular momentum loss proposed on theoretical grounds.

Subject headings : stars: activity – stars: evolution – stars: rotation – stars: spots – X-rays: stars

---

[1]Visiting Astronomer, Kitt Peak National Observatory, National Optical Astronomy Observatories, which is operated by the Association of Universities for Research in Astronomy, Inc. (AURA) under cooperative agreement with the National Science Foundation.

[2]Current address: JILA, Univ. of Colorado, Campus Box 440, Boulder, CO 80309

1. Introduction

Angular momentum evolution in stars is intimately related to the stellar magnetic field because protostars are thought to be magnetically coupled to circumstellar accretion disks and also because stars lose angular momentum in magnetized winds. The magnetic field is related to stellar activity, including coronal activity such as X-ray emission, chromospheric activity such as Hα and Ca II emission, and photometric variability due to star spots. Unfortunately, it is generally true that the stellar winds from low mass stars, the angular momentum loss, and even the magnetic field strength and structure are not directly observed. Observational studies of angular momentum evolution have therefore centered on correlations between stellar activity as indicators of magnetic activity, and other stellar properties such as mass, age and rotation rate.

The observed distributions of rotation velocities in open clusters of different ages reveal that the rate at which stars lose angular momentum on the main sequence depends both on their age and their mass (e.g., Stauffer 1991). The angular momentum loss rate, $\dot{J}$, is proportional to ωB^2 for low to moderate values of ω, where ω is the angular velocity and B is the mean surface magnetic field (Weber & Davis 1967). As B is proportional to ω for a linear dynamo, $\dot{J}$ is proportional to ω^3 for slow rotators. If this is also true for high values of ω, then rapid rotation would be suppressed prior to the main sequence as fast spinners would undergo heavy angular momentum loss (Pinsonneault, Kawaler, & Demarque 1990). The observation of rapid rotators on the main sequence in young open clusters such as α Per (50 Myr) and the Pleiades (70 Myr) (Stauffer et al. 1984; Stauffer et al. 1985; Stauffer 1994a) thus requires a saturation of $\dot{J}$ at high rotation rates in theories of angular momentum evolution. There is also some theoretical support for a decreased sensitivity of $\dot{J}$ to ω at higher rotation rates (Mestel & Spruit 1987; MacGregor & Brenner 1991).

It has long been known that chromospheric activity and X-ray activity are correlated with rotation among lower main-sequence stars, gradually increasing from the slow rotators to the rapid rotators and then reaching a plateau (Noyes et al. 1984; Rosner, Golub, & Vaiana 1985). This plateau is sometimes interpreted as due to a saturation in the mean surface magnetic field. The amplitude of brightness variations in low-mass stars has also been proposed as an alternate indicator of the saturation of the surface magnetic field (O'Dell et al. 1995).

There is considerable scatter in plots of stellar chromospheric and coronal activity vs. rotation which is greatly reduced if activity is plotted vs. the Rossby number, defined as the ratio of the rotation period (P_{rot}) to the convective overturn time (τ_{conv}) (Noyes et al. 1984; Simon, Boesgaard & Herbig 1985; Patten & Simon 1996). As τ_{conv} depends on mass, this suggests that stellar activity in stars depends both on rotation and on mass (e.g., Patten & Simon 1996).

Reproducing the mass-dependent rapid rotation and spindown has been a challenge for theoretical models until recently (see Krishnamurthi et al. 1997 for a review of theoretical efforts). Some models, using a constant value of the saturation threshold that depends only on the angular velocity, cannot reproduce the mass dependence of the rapid rotator phenomenon (e.g., Kawaler

1987, 1988, Chaboyer et al. 1995a, 1995b) while others suppress rapid rotation prior to the main sequence (e.g., Pinsonneault, Kawaler, & Demarque 1990).

Some recent models (Collier Cameron & Li 1994, Barnes & Sofia 1996) have considered a mass-dependent angular momentum loss law to explain the observed distribution of rotation velocities of open cluster stars. The models of Collier Cameron and Li (1994) have their starting point on the main sequence. They use an explicit mass dependence in the scaling constant in the angular momentum loss and a very high mass-dependent saturation threshold for $\dot{J}$ (45-75 $\omega_{\odot}$). However, given these parameters, Krishnamurthi et al. (1997) find that rapid rotation is suppressed prior to the main sequence for solar analogs with saturation thresholds greater than 20 $\omega_{\odot}$. Barnes & Sofia (1996) also note that different masses require different saturation thresholds in order to account for the ultra fast rotators in the young cluster data. However, they use an empirical fit for ω_{crit} as a function of mass. Recent models of angular momentum evolution by Krishnamurthi et al. (1997) successfully reproduce the observed distribution of rotation rates in open clusters of different ages by assuming the angular momentum loss saturation depends on the Rossby number (and hence mass), not angular velocity alone. As it is known that the same mass dependence reduces the scatter in the $P_{\rm rot}$-X-ray plane (Patten & Simon 1996), this establishes a connection between theory and observations that we explore further.

In this paper, we report new period measurements for 18 stars in the Pleiades, increasing the number of known rotation periods in this cluster to 51. The correlation between activity and rotation in the Pleiades and other open clusters has long been studied using $v \sin i$ measurements (e.g., Stauffer et al. 1994). As there is now a large sample of rotation periods in the Pleiades, the correlation can be studied free of ambiguities introduced by the unknown angle of inclination. We use this larger dataset of rotation periods to explore which measure of stellar activity is the best observational indicator of stellar magnetic field strengths and their saturation.

2. Data Acquisition and Analysis

As part of an ongoing program to determine the photometric rotation periods for stars in open clusters, we selected targets in the Pleiades spanning a range of magnitudes, from V=10 ($M \sim 1.0 M_{\odot}$) to V=16 ($M \sim 0.4 M_{\odot}$), in order to better define the correlation of activity indicators and rotation over a wide mass range. We obtained differential photometry for three sets of targets over three observing seasons (Oct. 1994-Jan. 1995, Oct. 1995-Jan. 1996, and Oct. 1996), using the Kitt Peak 0.9 m telescope, the 1.8 m and 1.1 m telescopes at Lowell Observatory in Flagstaff, the NURO 0.8 m telescope, also in Flagstaff, and the 1.2 m telescope at Mount Hopkins. Table 1 summarizes the characteristics of the various telescope and detector combinations. We opted to obtain differential photometry as this technique allowed us to utilize nights with marginal weather that made uniform absolute photometry difficult. This maximized the number of nights that could be used for observations. Each of the target fields was imaged in broadband V.

2.1. NURO data

The data obtained on the NURO 0.8m telescope was reduced separately as the field of view was very small ($4'$). The first step in the reduction of the NURO data was to remove the zero-read bias and to divide by a flatfield image. Aperture magnitudes were then used to derive the differential photometry from the reduced images. The instrumental magnitudes for the target star and the brightest nearby stars were derived using the routine APPHOT in the IRAF[1] package. The star aperture was set to have a radius of 1.5 times each night's average seeing FWHM, and the sky values measured in a contiguous annulus with a width of 1.5 FWHM. The difference in magnitude between the target and the comparison stars in the instrumental V band pass was then computed. These differential magnitudes were then used to compute the rotation period.

Here and for the observations made on other telescopes, we made no attempt to transform the magnitudes to a standard system. It was sometimes the case with the NURO data, particularly for the brightest targets, that the nearby comparison stars were much fainter than the target star. This meant that the differential magnitude of the target could not be determined with precision. For the 1994-1995 and 1995-1996 observing seasons, we typically used the NURO data in the determination of the rotation period when the uncertainties in the differential photometry were better than 0.025 mag on average. Only the NURO group obtained data during 1996. The targets selected for observation in 1996 were expected to have short rotation periods based on high $v \sin i$ values and on tentative period estimates for some of these stars from the 1994-95 observing run.

2.2. Other data

The data from the other telescopes were treated differently and we now describe this procedure. We began by doing the zero-exposure and flat field corrections, the latter from a combination of dome and sky flats when available. Rather than designating a set of predetermined comparison stars, we derived instrumental magnitudes for *all* stars on each reduced frame using version 2.0 of DoPhot (Schechter *et al.* 1993). We ignored all stars with central intensities which exceeded the linearity regime of the detector. This yielded the differential magnitudes of each target against all the remaining stars on each frame.

To assemble the photometry for each star into a time series, we first grouped the DoPhot output files by target star. Then for each target star, we first generated a time series for the observations from each telescope. The final step was to tie the observations on different telescopes together by using the conventional method of scaling the magnitudes against predetermined comparison stars. We did this by identifying 2-4 stars located near the target Pleiades member on the CCD chip with the smallest field of view. The scatter in the relative magnitudes of the

[1]The Image Reduction and Analysis Facility (IRAF) is distributed by the National Optical Astronomy Observatories, which is operated by AURA, Inc., under contract to the National Science Foundation.

comparison stars around their mean value gave an estimate of the accuracy of this process; normally the uncertainty was 0.01 mag or better. Then the offsets were computed to bring the comparison stars to the scale defined by the magnitude of the target star on the zero frame for that series. This offset was applied to all the magnitudes in the time series, thus rescaling the several time series to one common magnitude scale.

2.3. Determination of periods

We determined rotation periods using two different techniques. The first technique used the "Period" algorithm (Press et al. 1993) for the analysis of unevenly sampled time-series data. This routine also yields a measure of the false alarm probability (FAP) which indicates the significance of the derived period. A small value for the false alarm probability indicates a small probability that the peak is spurious (i.e due to random fluctuations).

The second technique used computes the best fitting sine wave to a given set of data. This routine utilizes the "Powell routine" (as described in Press et al. 1993) and computes the period based on the minimum chi-squared value. This routine also weights the data points by their photometric uncertainties. The uncertainty in the derived rotation period was computed to be the standard deviation of a Gaussian fit to the peak corresponding to the minimum chi-squared value. We used this routine to independently confirm our derived period. Both routines yielded the same period for the stars reported here.

Table 2 contains a summary of the observations, where the first column is the name of the star observed, column 2 is the number of observations per star, column 3 indicates the date/data range of the observations and column 4 specifies the telescope(s) used. Table 3 lists some properties of the stars we observed - column 2 is the V magnitude, column 3 is the $B-V$ color, column 4 is the $v \sin i$ measurement, if known, and column 5 is the logarithm of the X-ray luminosity of the stars normalized to the bolometric luminosity. Table 4 presents the newly determined periods; FAP represents the False Alarm Probability. The light curves are shown in Figure 1. We were successful in deriving periods for 21 of the 36 stars in our total sample. In addition to the new periods, we recovered periods for three known rapid rotators, Hii1883, Hii2244 and Hii2927. The values of 0.23d, 0.56d and 0.26d, respectively, agree with the previously determined values (van Leeuwen & Alphenaar 1982; Stauffer et al. 1987).

3. Indicators of magnetic field saturation

Chromospheric and coronal emission are often used as proxies for magnetic field strength. As mentioned earlier, these activity indicators are known to be correlated with rotation and are believed to saturate at some value of rotation. Armed with a considerably larger database of rotation periods in the Pleiades, we now re-examine plots of various activity indicators vs. the

rotation period.

O'Dell et al. (1995) examined rotation data for G and K single dwarfs with $0.55 \leq B-V \leq 1.40$. From a study of the amplitude of variation of the stellar brightness over one rotation period, ΔV, they concluded that ΔV increased with decreasing $P_{\rm rot}$ beyond the saturation threshold inferred from the chromospheric activity ($\sim$ 3 days for solar type stars, Vilhu 1984). They argued that the spot coverage continues to increase with increasing rotation rate, although the chromospheric activity appears to have saturated. They proposed that the amplitude of photometric variation might be a better indicator of the saturation of the magnetic field than the chromospheric activity, and derived an upper limit on the period for saturation at $P_{rot} \sim 12$ hours. We examine this by considering the dataset for the Pleiades, adding our new data to the sample, in the same color range.

As there are more X-ray data available for stars in open clusters, we start by plotting the chromospheric (Hα and Ca II) versus coronal (X-ray) activity indicators for stars in the Pleiades in Figure 2. This demonstrates that these activity indicators are indeed correlated with each other.

In Figure 3, we plot chromospheric Hα emission, the Ca II infrared triplet (data from Soderblom et al. 1993b), coronal X-ray emission (data from Micela et al. 1990 & Stauffer et al. 1994) and the amplitude of variation (compilation of older data (open circles) from O'Dell (1995); new data (filled circles) from this paper) for stars in the Pleiades against the rotation period. The amplitude of variation has been defined consistently in both datasets as the difference between the maximum and minimum magnitudes. The plot shows that the activity-rotation relations are similar for both chromospheric line emission and broadband X-ray emission, with an increase in activity levels towards decreasing P_{rot}. We note here that the trends for Hα and the Ca II lines appear to be have a more linear correlation with rotation than is seen in the X-ray data. However, more X-ray data are available in the Pleiades for stars with measured $P_{\rm rot}$, than Hα and Ca II data. The trends for all three indicators look very similar if the dataset for the X-ray emission is restricted to only those stars with measurements in the other two. The additional X-ray data helps to show a "saturation" type behaviour more clearly.

There is no trend seen for ΔV when our new rotation periods are included with the previously measured periods. It is also seen from the plot of ΔV against P_{rot} that higher amplitudes of variation exist at longer periods than seen previously (filled symbols in the range P_{rot}=2-10 days, $\Delta V \geq 0.1$ mag.). Thus ΔV does not increase with increasing rotation rates beyond the saturation limit of 3 days derived from chromospheric indicators (Vilhu 1984).

O'Dell et al. (1995) also noted that the coolest stars in their sample ($B-V >$1.15) had low amplitudes ($\Delta V <$0.12 mag) and speculated that this effect had some physical significance. In Figure 4, we plot amplitude vs. $B-V$ color including the uncertainty in the amplitude which is due to the uncertainty in the photometry. We find that four of the stars for which we have now measured P_{rot} in the Pleiades are cool stars with high amplitudes and this result is true even

when the uncertainty in the amplitudes is taken into account. Thus there does not appear to be a decrease in ΔV for cooler stars when the sample size is increased. Furthermore, the amplitude appears to vary at different epochs for a given star. Hii1883, the fastest rotator found to date in the Pleiades, has been monitored for over fifteen years. The amplitude of this star has been found to vary from 0.04 to 0.20 magnitudes over this time period (see Figure 13 in Soderblom et al. 1993a). Because three or four cycles of brightness modulation are required to be certain of the derived period, most reported periods for cluster stars are for rapid rotators (P_{rot} a fraction of a day to a couple of days) as they only need shorter observing runs to accurately measure a rotation period. Few stars with modest rotation periods (P_{rot} of 4 days and more) have had multiple amplitude measurements. By contrast, some of the rapid rotators have been studied over many years, and are therefore more likely to have light curves from several different epochs and may have been observed with a high amplitude in one of those epochs. In O'Dell et al. (1995), only the largest observed amplitude was selected for analysis. Hence, we conclude that the use of ΔV as an indicator of saturation of the magnetic field is ineffective.

4. Observational indicators of $\dot{\mathbf{J}}$

We know that both the chromospheric and coronal activity indicators are better correlated over a wide mass range with the Rossby number, N_R, than with rotation period alone. Hence, the saturation of the chromospheric and coronal emission depends both on rotation and mass (as the convective overturn time is a strong function of mass). Figure 5 illustrates this correlation for the Pleiades where the chromospheric activity indicators as well as $\log(L_x/L_{bol})$ are plotted against the inverse Rossby number, N_R^{-1}, calculated using theoretical convective overturn times from Kim & Demarque (1996). We also plot ΔV vs. the inverse Rossby number and note that this does not help to reduce the scatter. There does not appear to be a well-defined correlation between ΔV and P_{rot} or between ΔV and Rossby number for the Pleiades dataset.

Figure 5 shows that ΔV varies by a factor of ~ 6 for N_R^{-1}=10-100. This is comparable to the variation in ΔV at different epochs (a factor of $\sim$5) found by Soderblom et al. (1993a) for Hii1883. As X-ray activity in the Pleiades was studied by the *Einstein Observatory* and then by ROSAT a decade later, the scatter in X-ray activity with time for a star is observed to be a factor of at most $\sim$5 (Micela et al. 1996). Figure 5 shows that the range in X-ray activity for N_R^{-1}=10-100 is a factor of $\sim$40. Thus, while it is possible that ΔV depends on P_{rot} or N_R^{-1}, the dependence is masked by the scatter, unlike the X-ray activity.

As shown by Figure 5, the X-ray activity is very well correlated with the inverse Rossby number, plateauing at N_R^{-1} of ~ 20. In their theoretical models of angular momentum evolution in solar-type stars, Krishnamurthi et al. (1997) found that a mass-dependent angular momentum loss rate best reproduced the distribution of rotation rates seen in open clusters. The mass dependence used in their models was precisely this Rossby scaling. Thus, the Rossby number parameterizes the saturation threshold required both by theory (to explain the rotation distributions of open

clusters) and by observations (to best describe the X-ray and chromospheric activity). Hence, the saturation of X-rays in open cluster stars may be used as an observational indicator of the saturation of the angular momentum loss law. Identifying the precise level of X-ray saturation and its mass dependence will help to pin down the level at which the angular momentum loss saturates. This is crucial and should be a goal for ground-based and space-based studies to determine rotation periods and X-ray activity levels.

5. Conclusions

We have presented results of our photometric monitoring campaign of G, K and M dwarfs in the Pleiades. X-ray emission has long been known to correlate roughly with rotation period and has been shown to correlate well with Rossby number (defined as the ratio of the rotation period to the convective overturn time, hence a function of both rotation and mass). We conclude that the mass-dependent saturation of the X-ray emission is consistent with the mass-dependent saturation of the angular momentum loss required theoretically. Thus, we now have an observable that may be used to determine the threshold for angular momentum loss saturation. Additional periods and X-ray data obtained in the turnover region would aid in determining the functional form of the mass dependence. The lack of slowly rotating, cool, high amplitude variable stars in previous observations had led to some discussion on the use of the photometric amplitudes as an alternate diagnostic of saturation. However, our discovery of such stars in the Pleiades shows that the distribution of the amplitudes does not indicate a different saturation threshold than that inferred from X-rays.

The mass range of the stars included in our sample ranges from roughly 0.5-1.2 $M_{\odot}$. There is strong observational evidence that the mass dependence of the angular momentum loss law continues for lower mass stars (Stauffer et al. 1997; Jones, Fischer & Stauffer 1996). Establishing the mass dependence of the saturation in activity for the lower main sequence may provide valuable clues for models of stellar winds. In particular, there seems to be no obvious change in the rotation properties of stars at the boundary between stars with radiative cores and those which are fully convective ($\sim$0.25 $M_{\odot}$).

A Rossby-scaled angular momentum loss law would imply high saturation thresholds for stars more massive than 1.0 $M_{\odot}$, where the convective overturn timescale decreases rapidly with increasing mass. A loss law of the form used by Krishnamurthi et al. (1997) would suppress rapid rotation in higher mass stars. There is little evidence for angular momentum loss in either the pre-MS or the MS for stars with $M > 1.6$ $M_{\odot}$, while there is pre-main-sequence spindown in the intermediate-mass regime ($M \sim$ 1.3-1.6 $M_{\odot}$, Wolff & Simon 1997). The highest mass models (1.2 $M_{\odot}$) considered by Krishnamurthi et al. (1997) spun down too quickly when compared with the cluster data when a Rossby scaling for the saturation threshold was adopted. This may indicate either a change in the nature of the wind for stars of mass greater than 1 $M_{\odot}$ or a defect in the particular angular momentum loss prescription of Krishnamurthi et al. for high saturation

thresholds.

We close by noting that there are alternate means of limiting the angular momentum loss rates for rapid rotators. Buzasi (1997) has proposed a systematic tendency towards polar activity for lower mass stars as a possible explanation for the mass dependence of angular momentum loss (see also Solanki, Motamen & Keppens 1997). There are also other effects, for example a tendency towards a more complex magnetic field geometry at high field strengths, which could act to cap the angular momentum loss rates for rapid rotators (e.g., Mestel 1984). A good observational database of activity and rotation measurements as a function of mass and time may prove valuable for evaluating the relative merits of the different classes of theoretical models.

Observations were obtained with the Perkins 1.8m reflector of the Ohio Wesleyan and Ohio State Universities at Lowell Observatory, the 1.1m Hall telescope at Lowell Observatory, the 1.2m Mt. Hopkins telescope at Whipple Observatory and at the Lowell Observatory 0.8m telescope, which, under an agreement with Northern Arizona University and the NURO Consortium, is operated 60% of the time as the National Undergraduate Research Observatory. We thank the KPNO staff for their technical support during our runs on the 0.9m as well as R. Mark Wagner and Ray Bertram at Lowell Observatory for their technical support and expertise. We thank Jodie Dalton, Greg Piecuch and Phil Turcotte for assistance in observations at the NURO telescope as well as in reduction of the NURO data. We also wish to thank Charles Prosser at CfA for obtaining some measurements for this project and to Sidney Wolff for providing valuable comments. AK wishes to thank S.M. Long for discussions and help with the period-finding routines. Franklin and Marshall College and Gettysburg College thank the University of Delaware/Bartol Research Institute's NASA Space Grant College consortium for support of NURO membership and partial support of student travel. Financial support for this project was provided by NSF AST-9528227 to DT and MHP, an OSU Seed Grant to MHP and by NASA LTSA program grant NAGW-2698 to JRS.

We would also like to thank the anonymous referee for constructive comments which improved the paper significantly.

REFERENCES

Barnes, S., & Sofia, S. 1996, ApJ, 462, 746

Buzasi, D. L. 1997, ApJ, 484, 855

Collier Cameron, A., & Li, J. 1994, MNRAS, 269, 1099

Chaboyer, B., Demarque, P., & Pinsonneault, M. H. 1995a, ApJ, 441, 865

Chaboyer, B., Demarque, P., & Pinsonneault, M. H. 1995b, ApJ, 441, 876

Haro, G., Chavira, E., & Gonzalez, G. 1982, Boll. Obs. Tonantzintla y Tacubaya, 3, 3

Hempelmann, A., Schmitt, J. H. M. M., Schultz, M., Ruediger, G., & Stepien, K. 1995, A&A, 294, 515

Hertzsprung, E. 1947, Ann. Leiden Obs., 19, No. 1A

Jones, B. F., Fischer, D. A., & Stauffer, J. R. 1996, AJ, 112, 1562

Kawaler, S. D. 1987, PASP, 99, 1322

Kawaler, S. D. 1988, ApJ, 333, 236

Kim, Y. C., & Demarque, P. 1996, ApJ, 457, 340

Krishnamurthi, A., Pinsonneault, M. H., Barnes, S., & Sofia, S. 1997, ApJ, 480, 303.

Macgregor, K. B., & Brenner, M. 1991, ApJ, 370, L39

Magnitskii, A. K. 1987, SvAL, 13, 451

Mestel, L. 1984, in Cool Stars, Stellar Systems and the Sun, 3rd Cambridge Workshop, ed. S. L. Baliunas & L. Hartmann (Heidelberg: Springer-Verlag), 49

Mestel, L., & Spruit, H. C. 1987, MNRAS, 226, 57

Micela, G., Sciortino, S., Vaiana, G. S., Harnden, F. R. Jr., Rosner, R., & Schmitt, J. H. M. M. 1990, ApJ, 348, 557

Micela, G., Sciortino, S., Kashyap, V., Harnden, F. R. Jr., & Rosner, R. 1996, ApJS, 102, 75

Noyes, R. W., Hartmann, L. W., Baliunas, S. L., Duncan, D. K., & Vaughan, A. H. 1984, ApJ, 279, 763

O'Dell, M. A., Panagi, P., Hendry, M. A., & Collier Cameron, A. 1995, A&A, 294, 715

Patten, B., & Simon, T. 1996, ApJS, 106, 489

Pinsonneault, M. H., Kawaler, S., & Demarque, P. 1990, ApJS, 74, 501

Press, W. H., Teukolsky, S. A., Vetterling, W. T., & Flannery, B. P. 1993, in *Numerical Recipes*, p.569

Prosser, C. P. et al. 1993, PASP, 105, 1407

Prosser, C. P. et al. 1995, PASP, 107, 211

Rosner, R., Golub, L., & Vaiana, G. S. 1985, ARAA, 23, 413

Schechter, P. L., Mateo, M., & Saha, A. 1993, PASP, 105, 1342

Simon, T., Boesgaard, A. M., & Herbig, G. 1985, ApJ, 293, 551

Soderblom, D. R., Stauffer, J. R., Hudon, J. D., & Jones, B. F. 1993a, ApJS, 85, 315

Soderblom, D. R., Jones, B. F., Balachandran, S., Stauffer, J. R., Duncan, D. K., Fedele, S. B., & Hudon, J. D. 1993b, AJ, 106, 1059

Solanki, S. K., Motamen, S., & Keppens, R. 1997, A&A, 325, 1039

Stauffer, J. R. 1984, ApJ, 280, 202

Stauffer, J. R. 1985, ApJ, 289, 247

Stauffer J. R., Schild, R. A., Baliunas, S. L., & Africano, J. L. 1987b, PASP, 99, 471

Stauffer, J., Klemola, A., Prosser, C., & Probst, R. AJ, 101, 980

Stauffer, J.R. 1991, in Angular Momentum Evolution in Young Stars, Dordrecht: Kluwer, ed. Catalano & Stauffer, NATO ASI Series, 340

Stauffer, J. R. 1994a, in Cool Stars, Stellar Systems and the Sun, 8th Cambridge Workshop, ASP Conf. Ser., Vol. 64, San Francisco:ASP, ed. J. -P. Caillault, 163

Stauffer, J. R., Caillault, J. -P., Gagne, M., Prosser, C. P., & Hartmann, L. W. 1994, ApJS, 91, 625

Stauffer, J. R., Balachandran, S. C., Krishnamurthi, A., Pinsonneault, M., Terndrup, D. M., & Stern, R. A. 1997, ApJ, 475, 604.

van Leeuwen, F. & Alphenaar, P. 1982, ESO Messenger No. 23, p. 15 (VA)

Vilhu, O. 1984, A&A, 133, 117

Weber, E. J., & Davis, L. Jr. 1967, ApJ, 148, 217

Wolff, S. C., & Simon, T. 1997, PASP, 109, 759

Fig. 1.— Differential light curves in V for Pleiades stars. The different symbols indicate data taken on different telescopes. The crosses are data from the KPNO 0.9m telescope, the open circles are from the SAO 1.2m telescope, the filled triangles are from the 1.8m Perkins telescope, the open triangles are from the 1.8m Perkins telescope in 2×2 binned mode, the stars are from the NURO 0.8m telescope and the squares are from the 1.1m Hall telescope. The error bars indicate the photometric uncertainties.

Fig. 2.— Correlation of chromospheric and coronal activity indicators for available data in the Pleiades. (top) The ratio of the Hα flux to the stellar bolometric flux, R(Hα), vs. the X-ray luminosity normalized to the bolometric luminosity, (L_x/L_{bol}). (bottom) The ratio of the flux in the 8542Å line of Ca II to the bolometric flux, R[Ca II(8542)] vs. (L_x/L_{bol}). Hα and Ca II data from Soderblom et al. (1993b); X-ray data from Stauffer et al. (1994).

Fig. 3.— Activity indicators for Pleiades stars vs. rotation period, P_{rot}. (top) Chromospheric Hα emission and Ca II infrared triplet at 8542Å . (bottom) The X-ray luminosity normalized to the bolometric luminosity, L_x/L_{bol}, and the amplitude of variation at V due to starspot modulation, ΔV. Hα, CaII and X-rays increase with decreasing rotation period. Hα and Ca II data from Soderblom et al. (1993b); X-ray data from Stauffer et al. (1994). Rotation period data: *Open symbols* - Previously existing periods from Magnitskii (1987), Stauffer et al. (1987), Prosser *et al.* (1993) and Prosser et al. (1995), as compiled by O'Dell et al. (1995). *Filled symbols* - Our new periods.

Fig. 4.— The amplitude of photometric variation, ΔV, vs. $B-V$ color for Pleiades stars. *Open symbols*: Periods compiled by O'Dell et al. (1995). *Filled symbols*: Our new periods. Error bars represent the uncertainty in the amplitude determination due to the photometric uncertainties.

Fig. 5.— Activity indicators for Pleiades stars vs. the log of the inverse Rossby number, P_{rot}/τ_{conv}, where τ_{conv} is the convective overturn timescale. (top) Chromospheric Hα emission and Ca II infrared triplet at 8542Å, (bottom) (L_x/L_{bol}) and ΔV. Symbols represent same as in Fig. 3.

TABLE 1
TELESCOPES AND DETECTORS

Telescope	Scale ($''$/pix)	FOV($'$)	Gain(e^-/DN)	RN (DN)	Linearity (DN)
NURO 0.8m	0.49	4.0	12.9	10.5	20,000
KPNO 0.9m	0.68	23.0	3.2	4.0	180,000
Lowell 1.1m	0.38	5.0	2.3	9.0	18,000
SAO 1.2m	0.65	11.0	2.8	13.0	30,000
Lowell 1.8m	0.50	6.7	1.5	12.0	30,000

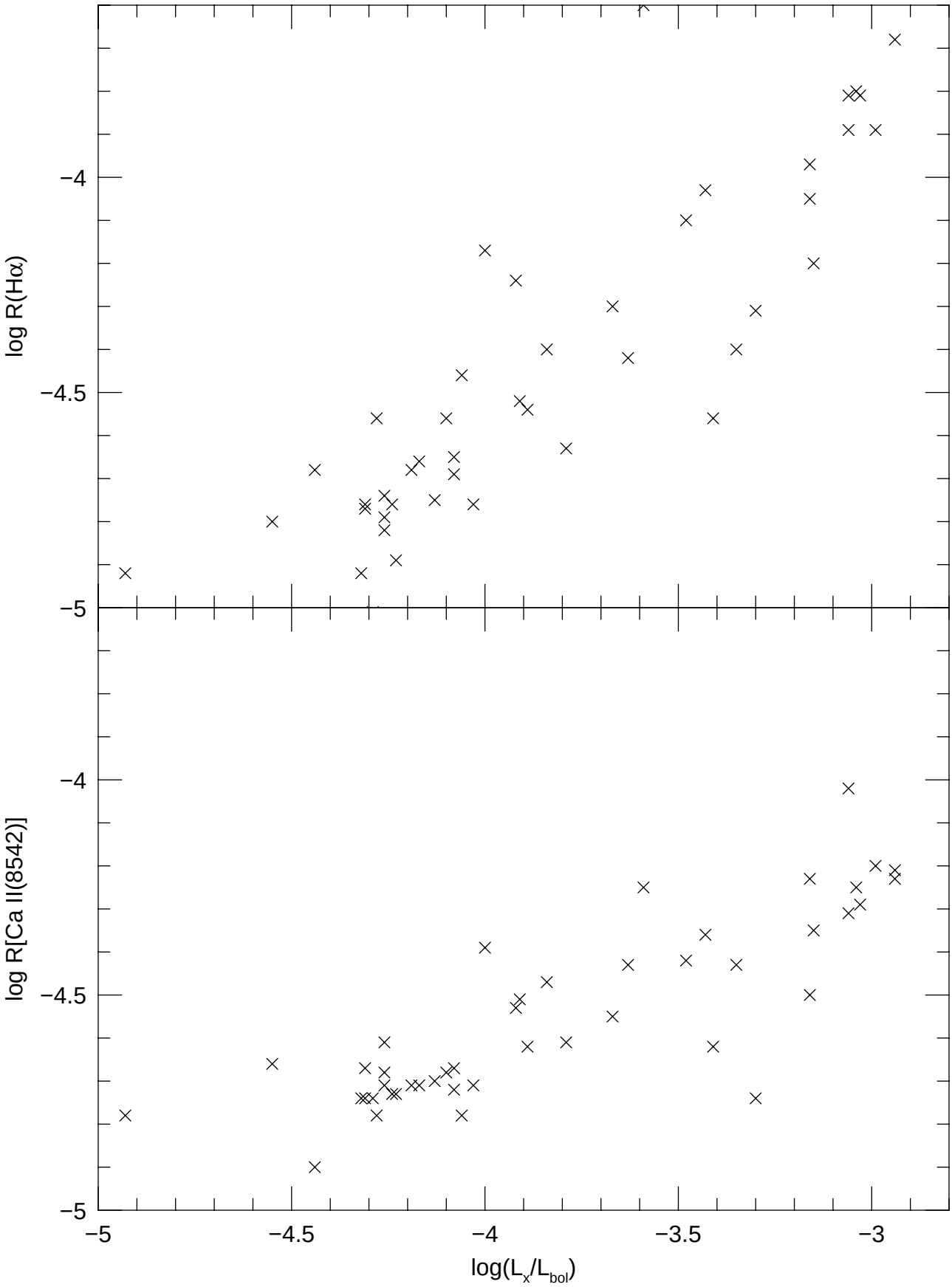
log R(Hα)
−4
−4.5
−5
log R[Ca II(8542)]
−4
−4.5
−5
−5
−4.5
−4
−3.5
−3
log(L_x/L_bol)

TABLE 2
SUMMARY OF OBSERVATIONS

Star[a]	N_{obs}	Dates of obs.	Telescope[b]
Hcg20	40	Oct94-Dec94	1,2,3,4,5
Hcg44	28	Oct94-Dec94	2,3,4,5
Hcg71	52	Nov95-Dec95	2,5
Hcg77	38	Oct94-Dec94	1,2,3,4,5
Hcg103	27	Oct94-Dec94	2,3,4,5
Hcg195	27	Oct94-Dec94	1,2,3,4,5
Hcg219	31	Oct94-Dec94	2,3,4,5
Hcg380	26	Nov95-Dec95	2,5
Hcg422	26	Nov95-Dec95	2,5
Hii133	61	Nov95-Dec95	2,4,5
Hii174	38	Oct96	1
Hii191	43	Nov95-Dec95	2,4,5
Hii212	41	Nov95-Dec95	2,5
Hii253	37	Oct96	1
Hii263	54	Oct94-Dec94	1,2,3,4,5
Hii345	34	Oct96	1
Hii708	37	Oct96	1
Hii738	37	Oct96	1
Hii793	37	Nov95-Dec95	2,4,5
Hii883	37	Oct94-Dec94	1,2,3,4,5
Hii930	63	Nov95-Dec95	2,4,5
Hii1029	26	Nov95-Dec95	2,5
Hii1032	34	Oct96	1
Hii1280	32	Nov95-Dec95	2,5
Hii1305	32	Oct96	1
Hii1512	32	Oct94-Dec94	1,2,3,4,5
Hii1532	36	Oct96	1
Hii1553	36	Oct96	1
Hii1653	36	Oct96	1
Hii1883	47	Oct94-Dec94	1,2,3,4,5
	38	Oct96	1
Hii2147	37	Oct96	1
Hii2244	47	Oct94-Dec94	1,2,3,4,5
	37	Oct96	1
Hii2786	34	Oct96	1
Hii2927	52	Oct94-Dec94	1,2,3,4,5
Hii2966	43	Nov95-Dec95	2,5
Hii3197	37	Oct96	1

[a]Hii refers to the second list in Hertzsprung 1947, sometimes also referred to as Hz; Hcg refers to the catalog of Haro, Chavira & Gonzalez 1982

[b]1: NURO 0.8m, 2: KPNO 0.9m, 3: Lowell 1.1m, 4: SAO 1.2m, 5: Lowell 1.8m

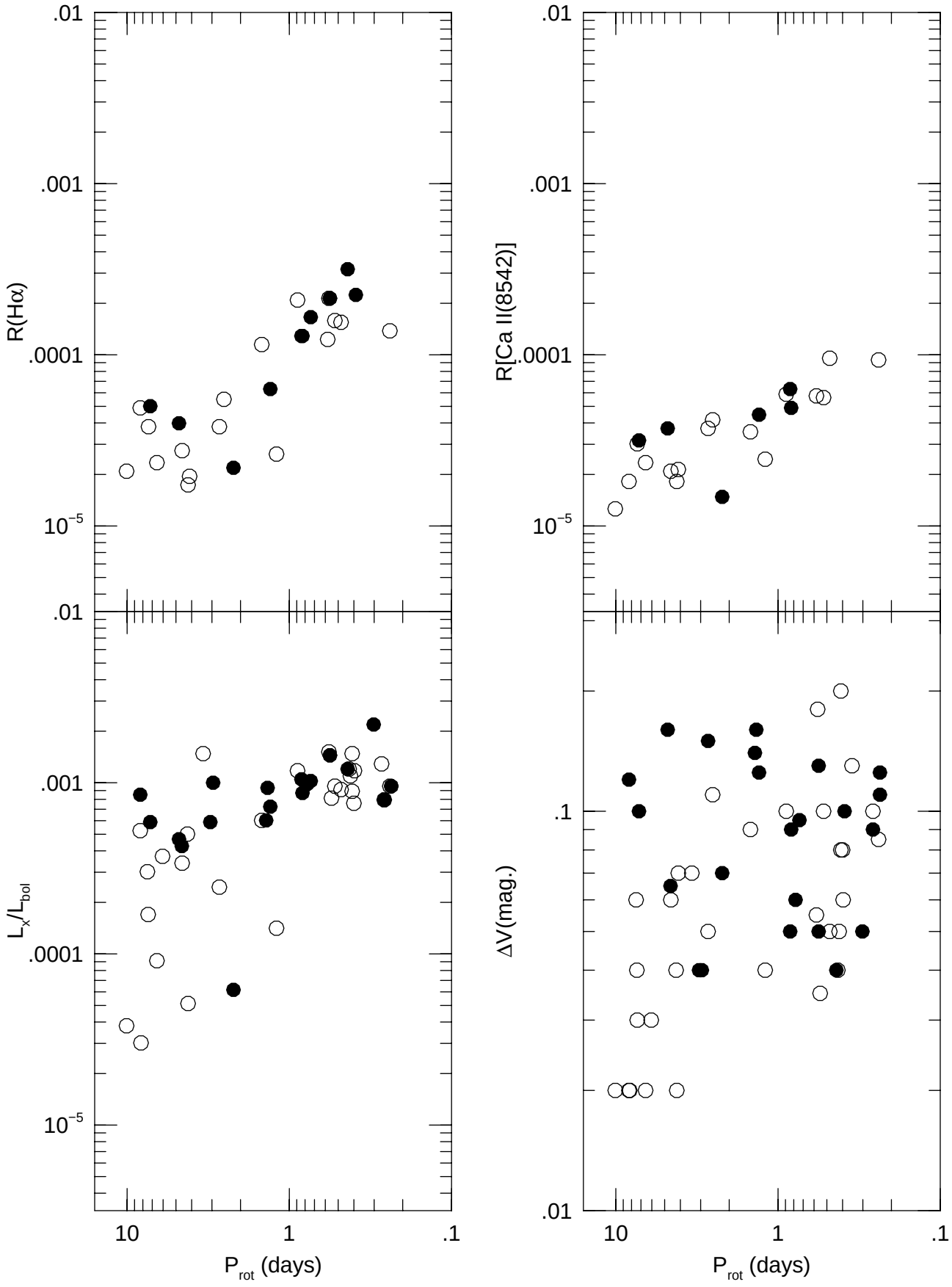
.01
.001
.0001
10^{-5}
R(Hα)
.01
.001
.0001
10^{-5}
R[Ca II(8542)]
.001
.0001
10^{-5}
L_x/L_{bol}
.1
.01
ΔV(mag.)
10
1
.1
P_{rot} (days)
10
1
.1
P_{rot} (days)

TABLE 3

PROPERTIES OF THE OBSERVED STARS

Star	V[a]	$B-V$[a]	$v \sin i$[b](km s^{-1})	Log(L_x/L_{bol})[c]
Hcg20	14.23	1.37	···	···
Hcg44	16.15	···	···	···
Hcg71	14.36	1.37	···	−3.23
Hcg77	15.16	1.50	···	···
Hcg103	16.05	···	···	−3.28
Hcg195	15.30	1.47	···	···
Hcg219	15.83	1.05	···	−3.11
Hcg380	16.14	1.48	···	−3.24
Hcg422	16.06	···	···	−2.54
Hii133	14.14	1.31	19	−3.03
Hii174	11.62	0.81	28	−2.94
Hii191	14.38	1.31	···	−3.00
Hii212	14.18	1.33	10	−3.06
Hii253	10.66	0.65	37	−3.01
Hii263	11.63	0.88	10	−3.33
Hii345	11.57	0.81	18	−2.98
Hii708	10.13	0.58	46	−3.89
Hii738	12.30	0.81	50	−3.06
Hii793	14.15	1.43	<9	−3.96
Hii883	13.05	1.08	6:[e]	< -3.23[d]
Hii930	14.08	1.22	20	−3.22
Hii1029	13.52	1.35	···	−3.88
Hii1032	11.10	0.73	36	−3.14
Hii1280	14.44	1.40	···	−2.66
Hii1305	13.52	1.15	84	···
Hii1512	13.51	1.26	9	< -3.07[d]
Hii1532	13.05	1.08	6:[e]	−3.01
Hii1553	12.49	1.08	12	···
Hii1653	13.50	1.18	21	−2.99
Hii1883	12.66	1.03	140	< -3.02[f]
Hii2147	10.83	0.78	27	−2.83
Hii2244	12.58	0.99	50	−2.82
Hii2786	10.31	0.56	25	−4.21
Hii2927	13.97	1.26	90	−3.10
Hii2966	14.74	1.46	<9	−3.37
Hii3197	12.10	1.07	33	−2.92

[a]Stauffer et al. 1991

[b]Soderblom et al. 1993a

[c]Stauffer et al. 1994, unless otherwise indicated

[d]Micela et al. 1990

[e]indicates an uncertain value

[f]Hempelmann et al. 1995

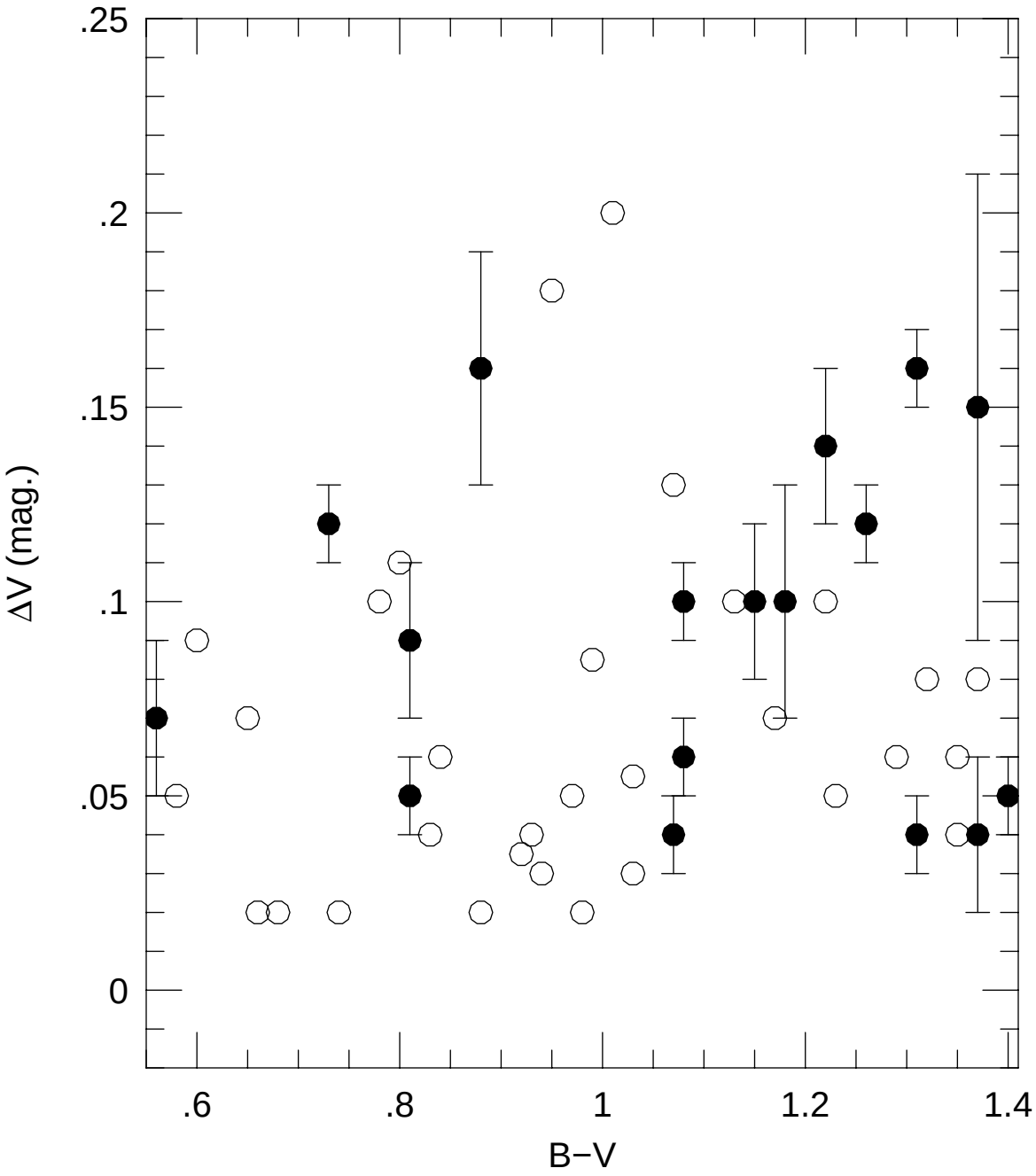
.25
.2
.15
.1
.05
0
ΔV (mag.)
.6
.8
1
1.2
1.4
B−V

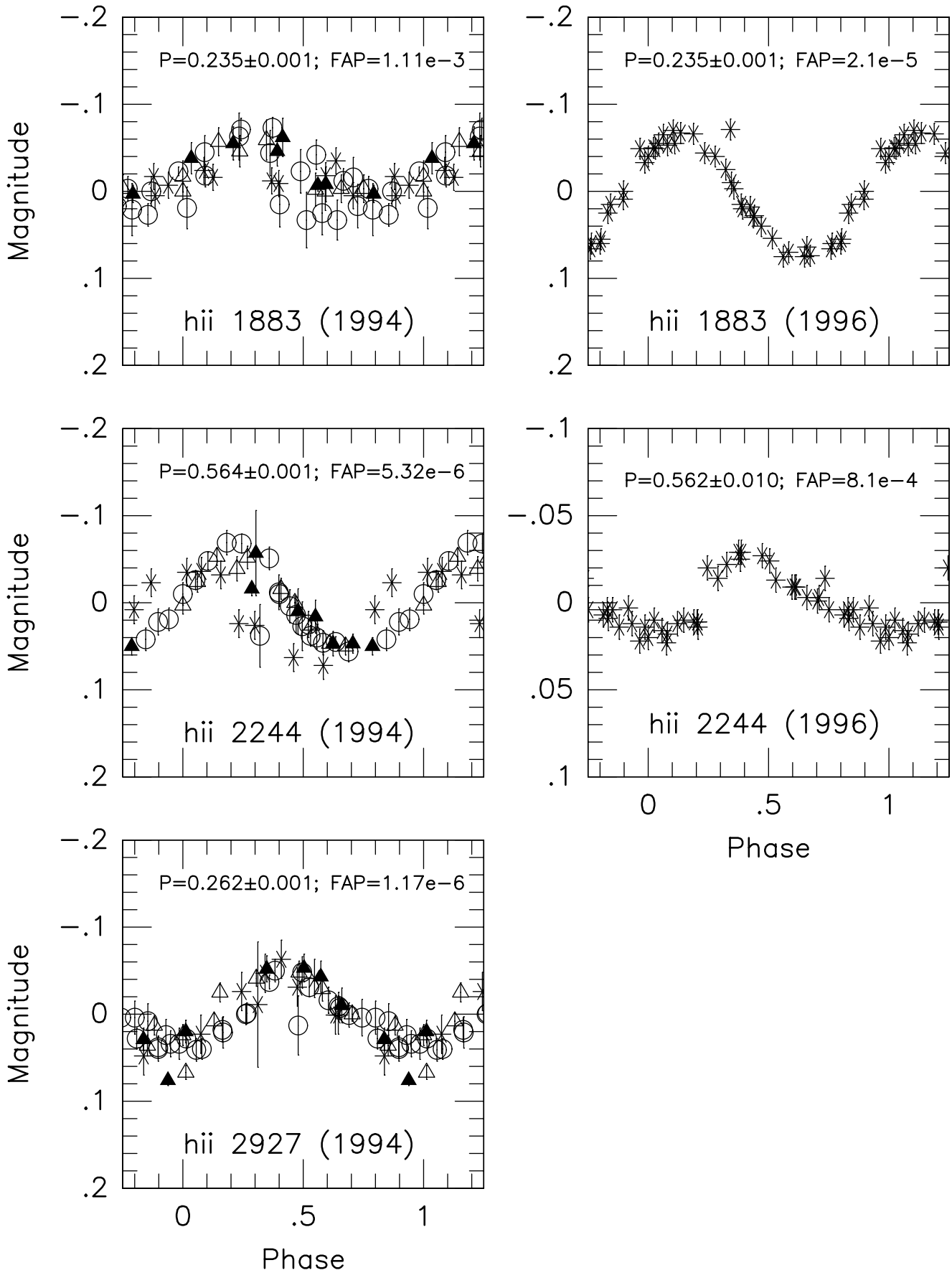
P=0.235±0.001; FAP=1.11e−3
hii 1883 (1994)
P=0.235±0.001; FAP=2.1e−5
hii 1883 (1996)
P=0.564±0.001; FAP=5.32e−6
hii 2244 (1994)
P=0.562±0.010; FAP=8.1e−4
hii 2244 (1996)
P=0.262±0.001; FAP=1.17e−6
hii 2927 (1994)
Magnitude
Phase
−.2
−.1
0
.1
.2
−.05
.05
.5
1

TABLE 4
NEW PERIODS REPORTED IN THIS PAPER

Star	Period (days)	Uncertainty (days)	ΔV (mag.)	Uncertainty in ΔV (mag.)	FAP
Hcg20	2.70	0.05	0.15	0.06	2.3e-4
Hcg71	2.98	0.08	0.04	0.02	7.1e-4
Hii133	1.36	0.01	0.16	0.01	2.9e-9
Hii191	3.1	0.9	0.04	0.01	5.2e-3
Hii263	4.82	0.17	0.16	0.03	1.1e-5
Hii345	0.84	0.02	0.05	0.01	5.1e-4
Hii738	0.83	0.02	0.09	0.02	5.5e-4
Hii883	7.2	0.4	0.10	0.01	1.2e-2
Hii930	1.39	0.01	0.14	0.02	2.3e-9
Hii1032	1.31	0.03	0.12	0.01	1.1e-4
Hii1280	0.302	0.001	0.05	0.01	1.1e-3
Hii1305	0.389	0.002	0.10	0.02	1.7e-4
Hii1512	8.2	0.2	0.12	0.01	5.3e-3
Hii1532	0.78	0.02	0.06	0.01	5.1e-3
Hii1653	0.74	0.02	0.10	0.03	3.4e-3
Hii2786	2.21	0.13	0.07	0.02	8.5e-4
Hii2966	4.6	0.4	0.07	0.02	2.2e-3
Hii3197	0.44	0.01	0.04	0.01	2.3e-3

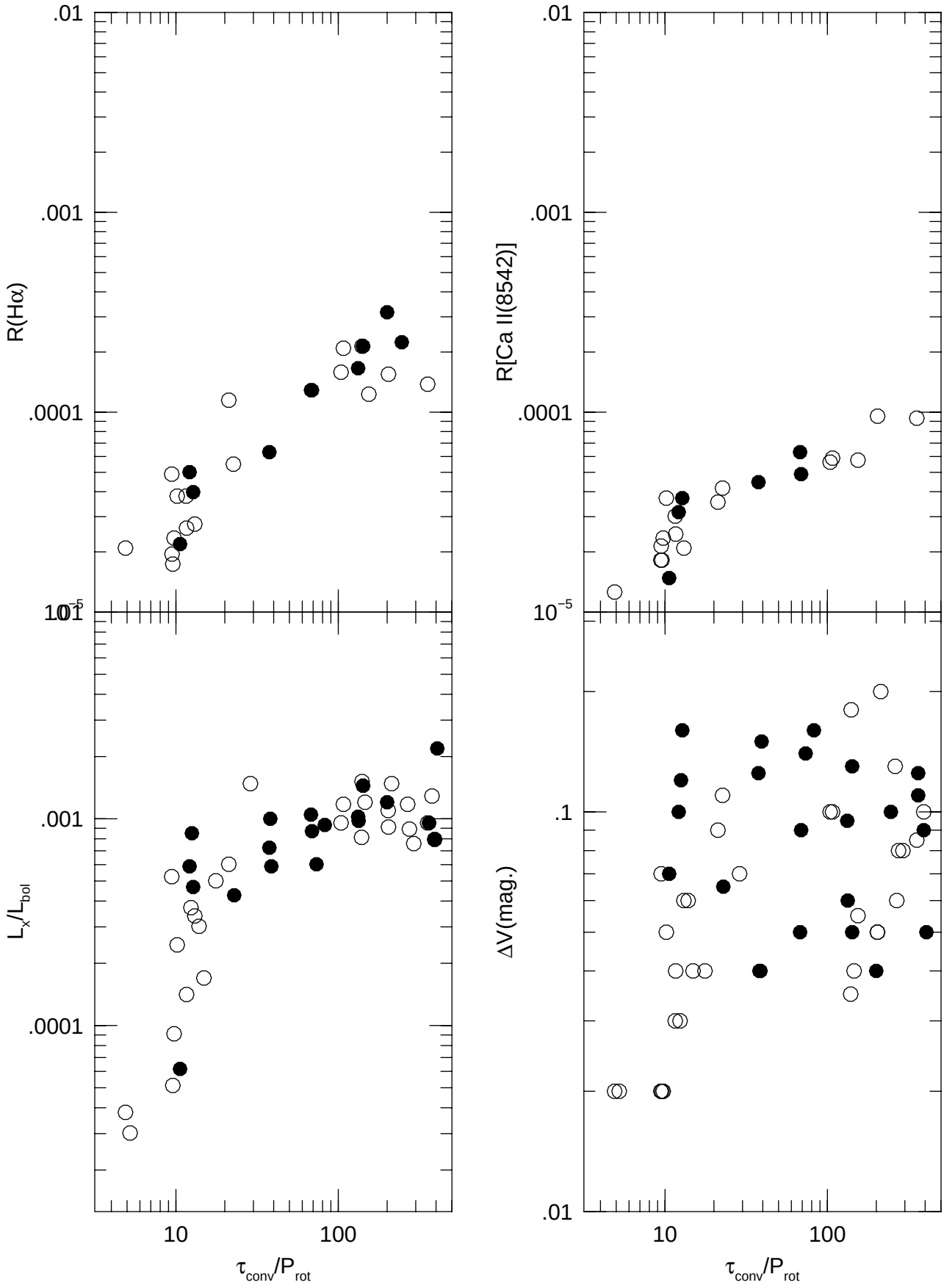
.01
.001
.0001
10^{-5}
R(Hα)
R[Ca II(8542)]
L_x/L_{bol}
ΔV(mag.)
.1
10
100
τ_{conv}/P_{rot}

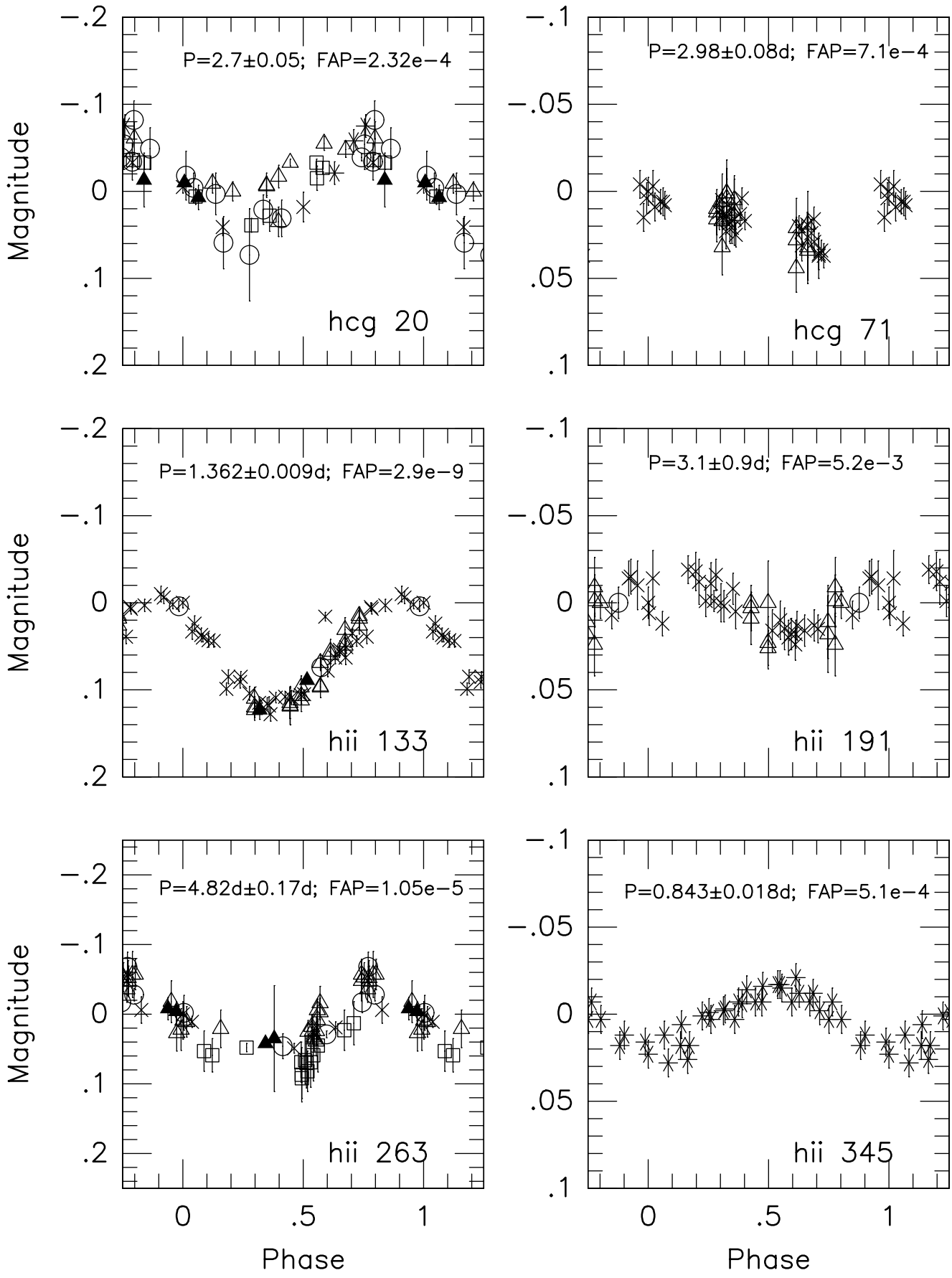
P=2.7±0.05; FAP=2.32e−4
hcg 20
P=2.98±0.08d; FAP=7.1e−4
hcg 71
P=1.362±0.009d; FAP=2.9e−9
hii 133
P=3.1±0.9d; FAP=5.2e−3
hii 191
P=4.82d±0.17d; FAP=1.05e−5
hii 263
P=0.843±0.018d; FAP=5.1e−4
hii 345
Magnitude
Phase
−.2
−.1
0
.1
.2
.05
.5
1

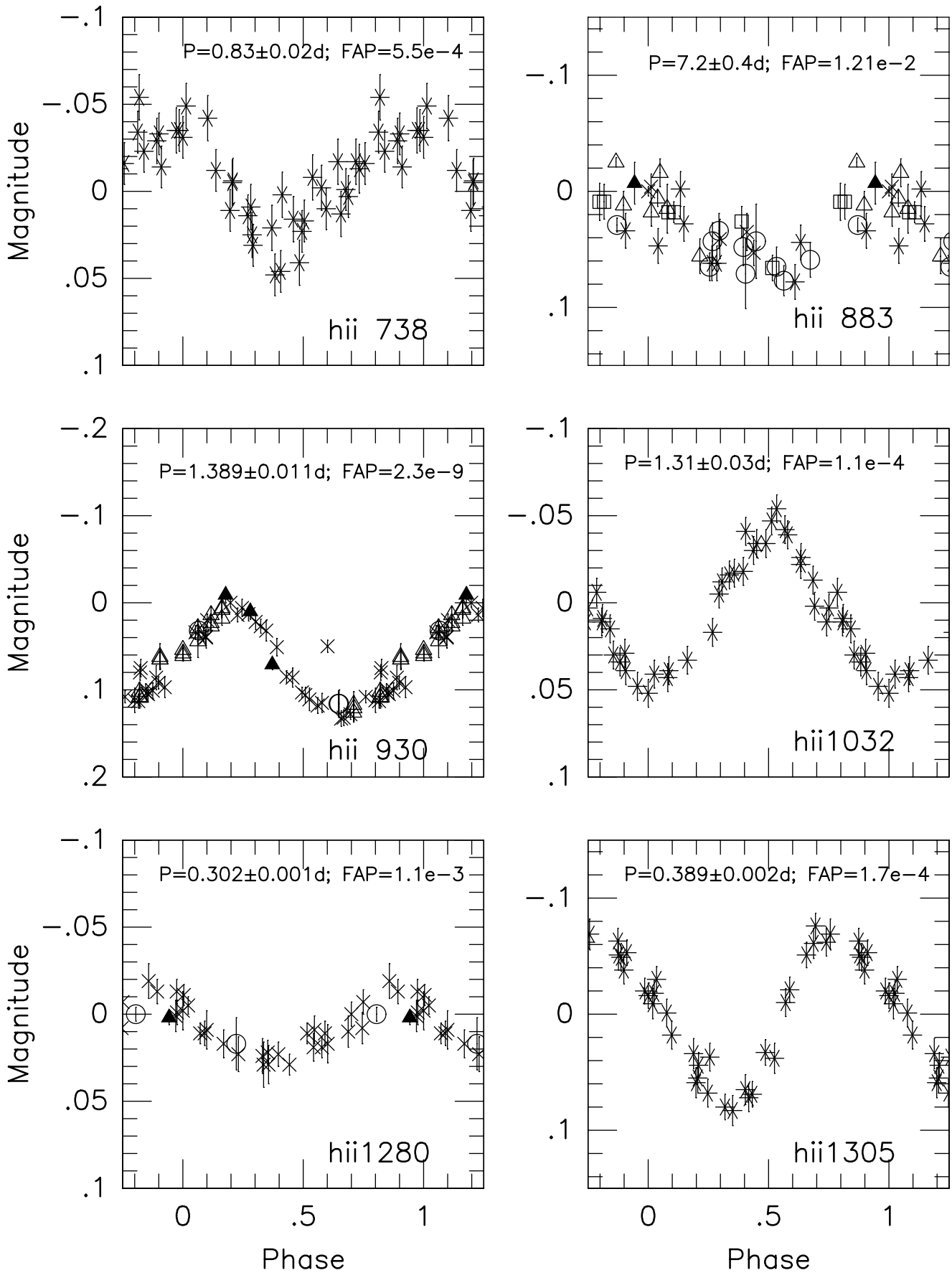
P=0.83±0.02d; FAP=5.5e−4
hii 738
P=7.2±0.4d; FAP=1.21e−2
hii 883
P=1.389±0.011d; FAP=2.3e−9
hii 930
P=1.31±0.03d; FAP=1.1e−4
hii1032
P=0.302±0.001d; FAP=1.1e−3
hii1280
P=0.389±0.002d; FAP=1.7e−4
hii1305
Magnitude
Phase

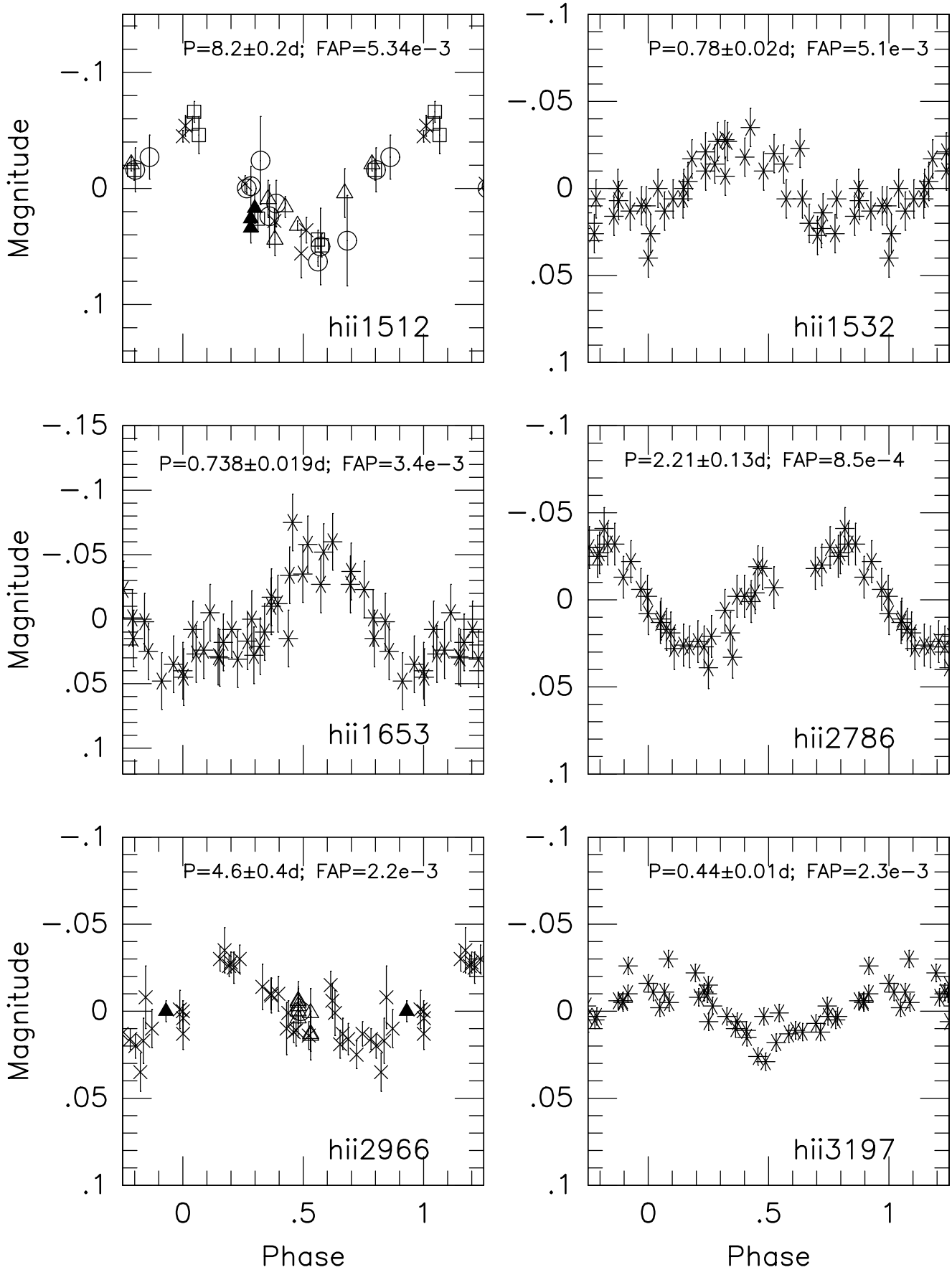
P=8.2±0.2d; FAP=5.34e−3
hii1512
P=0.78±0.02d; FAP=5.1e−3
hii1532
P=0.738±0.019d; FAP=3.4e−3
hii1653
P=2.21±0.13d; FAP=8.5e−4
hii2786
P=4.6±0.4d; FAP=2.2e−3
hii2966
P=0.44±0.01d; FAP=2.3e−3
hii3197
Magnitude
Phase
−.15
−.1
−.05
0
.05
.1
.5
1